Amplitude dependence of elasticity for the assembly of SiO₂ powders under shear oscillation strain

X. M. Xiong and J. X. Zhang

State Key Laboratory of Optoelectronic Materials and Technologies, School of Physics & Engineering, Sun Yat-Sen University,
Guangzhou 510275, People's Republic of China

We experimentally report the elastic response of an assembly of SiO₂ powders under a shear oscillation strain by a modified inverted torsion pendulum with a Couette-like setup. We find that the shear restoring force displayed by SiO₂ assembly is of strong amplitude dependence, which is ascribed to the dynamic behavior of the stress network inside and could be used to classify the states of the SiO₂ assembly, i.e., elastic solid, plastic solid, viscoelastic solid, and viscous fluid. The underlying mechanisms for different states of the SiO₂ assembly are tentatively proposed.

Granular material is ubiquitous and is regarded as a fourth state of matters, different from the normal solid, liquid and gas. It is inherently dissipative and displays solid-like, liquid-like or gas-like behavior, depending on the external condition, and attracts a growing interest in past decades due to its rich phenomenology and important applications [1]. In its static state, granular material shows inhomogeneous spatial stress profiles called stress (force) network, which are primarily carried by a fraction of the total number of grains [2]. Despite of extensive investigations the stress network is still illusive and the static granular material shows intriguing properties [3].

In this Brief report, we put forward a method to investigate the elastic response of static granular material under shear oscillation strain by making use of a modified inverted torsion pendulum with a Couette-like setup. And we find that the assembly of SiO₂ powders displays an unexpected amplitude dependence of elasticity under shear oscillation strain, from which we could infer the state of the stress network inside the assembly of SiO₂ powders and its evolution with the increase in shear oscillation strain amplitude.

By attaching a Couette-like setup onto the conventional inverted torsion pendulum, we develop a viscoelastic spectroscope for granular material [4] shown schematically in Fig. 1. In the absence of granular material, the viscoelastic spectroscope is essentially a conventional inverted torsion pendulum and can undertake a forced torsion vibration under an external periodical torque produced by the current flowing through the coils [5]. The forced torsion vibration could be described by the following equation:

$$I\ddot{\theta} + (k_1 + ik_2)\theta = F_0 e^{i\omega t}, \qquad (1)$$

where I is the moment of inertia of the torsion pendulum, θ is the vibration angle, while k_1 and k_2 are the restoring (elastic) and dissipative torque coefficient due to the twisting element, respectively. $F_0 e^{i\omega t}$ represents an external oscillation torque, where $\omega = 2\pi f$ is the circle frequency. In its steady solution, the vibration angle $\theta = \theta_0 e^{i(\omega t - \delta)}$ lags behind the external torque by a phase angle δ. Further calculation shows that the phase angle δ has the following frequency dependence [6]:

$$tg\,\delta = \frac{\omega_r^2 k_2}{k_1(\omega_r^2 - \omega^2)}, \qquad (2)$$

where $\omega_r = 2\pi f_r = \sqrt{k_1/I}$ is the system resonant circle frequency, and we call tan δ the apparent internal friction. While we continuously vary the frequency of the external torque across the system resonant frequency, the phase angle δ changes from a small value (k_2/k_1) to a large value (about π) crossing the value of $\pi/2$ with an abrupt change at the system resonant frequency f_r. So the tan $\delta \sim f$ plot shows a hyperbolic divergence at the system resonant frequency f_r, from which we can experimentally determine f_r with a very high precision. And then we could readily obtain the moment of inertia of the system via $I = k_1/(2\pi f_r)^2$ while the restoring (elastic) torque coefficient k_1 is calculated from the geometry of the twisting element.

After filling an assembly of granular material into the Couette container, the torsion vibration of the viscoelastic spectroscope could be described by the following equation
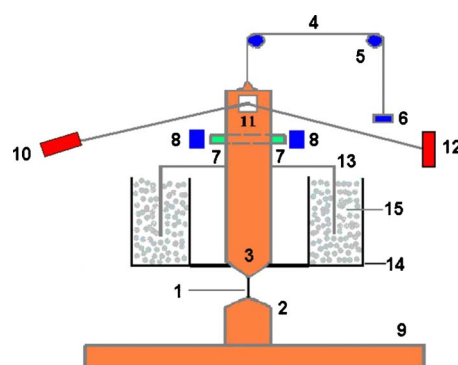

FIG. 1. (Color online) Schematic diagram of viscoelastic spectroscope for granular material. (1) solid specimen (copper wire with $\phi = 0.8$ mm and $l = 32$ mm); (2) fixed grip; (3) rotational grip and torsion rod; (4) weak suspension; (5) pulleys; (6) counterweight; (7) magnet; (8) pair of driving coils; (9) base; (10) lamp unit with blade slit; (11) mirror; (12) differential photocell; (13) rotational cylinder ($\phi = 35$ mm, $H = 40$ mm, made of aluminum); (14) double-layer container (with inner diameter of 10 mm and outer diameter of 60 mm); (15) granular material.

with the additional viscoelasticity terms due to the assembly of granular material:

$$I\ddot{\theta} + [(k_1 + k_{1G}) + i(k_2 + k_{2G})]\theta = F_0 e^{i\omega t}, \quad (3)$$

where k_{1G} and k_{2G} represent the shear elastic and dissipative torque coefficient of granular material respectively. In a similar way we also have

$$tg\,\delta = \frac{\omega_r'^2 (k_2 + k_{2G})/(k_1 + k_{1G})}{\omega_r'^2 - \omega^2}, \quad (4)$$

where the system resonant frequency $\omega_r' = 2\pi f_r' = [(k_1 + k_{1G})/I]^{1/2}$, different from the case for the absence of granular material due to the shear elasticity of granular material. Similarly the system resonant frequency f_r' could also be inferred from the tan $\delta \sim f$ plot as above discussions. And then we could obtain the total shear elasticity $k_1 + k_{1G} = (2\pi f_r')^2 I$. The shear elasticity coefficient of granular material could be obtained via the following formula:

$$k_{1G} = [(2\pi f_r')^2 - (2\pi f_r)^2]I. \quad (5)$$

In our inverted torsion pendulum based viscoelastic spectroscope [7], we could measure a broad frequency spectrum for tan δ where frequency range is from 0.01 Hz to 300 Hz with a high-frequency resolution of 0.01 Hz and well covers the system resonant frequency of about 100Hz, which depends on the elastic coefficient of the twisting element. At the same time, the amplitude of the torsion vibration angle could be controlled precisely via changing the torque amplitude. This means that we could precisely control the amplitude of shear oscillation strain imposed onto the granular assembly via the rotational cylinder, which is proportional to the amplitude of the torsion vibration angle. Furthermore, the amplitude of shear oscillation strain could be varied from several nanometers to hundreds micrometers. In this way we could conveniently investigate the shear elasticity of the granular material under different shear oscillation strain amplitudes.

We apply a copper wire with 0.8 mm in diameter and 32 mm in length as a twisting element in our experiments. So the elastic coefficient of the copper wire $k_1 = 6.5 \times 10^{-2}$ Nm. Figure 2 shows the plot of tan $\delta \sim f$ for the case without granular material, from which we could see that the system resonant frequency is 68.1 Hz. The moment of inertia of the viscoelastic spectroscope is 3.55×10^{-7} m Kg according to the formula $I = k_1/(2\pi f_r)^2$.

SiO$_2$ powders is bought commercially (Made in Qingdao Haiyang Chemical Co. Ltd. China) and has a narrow size distribution with a mean size of about 31 μm. Before experiment, both side (inner and outer) surfaces of rotational cylinder are cohered with a layer of SiO$_2$ powders, respectively. The SiO$_2$ powders are filled into the double-layer container of the Couette-like setup to a height of 16 mm. The container diameter (with an inner diameter of 10 mm and an outer diameter of 60 mm) is much larger than the average diameter of SiO$_2$ grains, making the arching effect vanish according to Kiwing et al. [8]. Prior to the experiments, the assembly of SiO$_2$ powders is stabilized by the following procedure. First, the container is tapped slightly for about 30–50
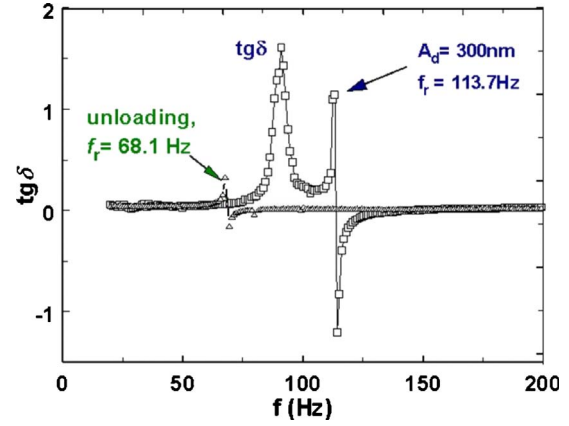

FIG. 2. (Color online) Frequency dependence of apparent internal friction tan δ of the system loaded and unloaded with SiO$_2$ powders. Triangles "$\triangle$" symbolize the tan δ of the unloaded system and squares "$\square$" denote the tan δ of the loaded system while the oscillation strain amplitude being 300 nm.

times at different points of the container to minimize the powder volume. Then the assembly of SiO$_2$ powders is subjected to a shear oscillation strain through the rotational cylinder with the amplitudes of 1 mm at the frequency of 70 Hz for over 30 min. Finally, the applied shear oscillation strain amplitude decreases from 1 mm to 10 nm in the period of about 1 h. According to the report of Nowak et al. [9], the assembly of SiO$_2$ powders can reach a reproducible steady state. In addition, during the experiment the room temperature is kept at 26 °C via the air conditioner and the humidity is about 50%.

Under constant oscillation amplitude of shear strain 300 nm, it is noticed that, in the presence of SiO$_2$ powders the pendulum resonance frequency $f_r = 113.7$ Hz is much higher than that without SiO$_2$ powders $f_r^o = 68.1$ Hz, as shown in Fig. 2. Meanwhile, one strong resonant absorption peak at about 92 Hz is readily observed, which is believed due to the microcavity structure inside the assembly of SiO$_2$ powders and required further investigations.

We change the amplitude of the shear oscillation strain imposed onto the assembly of SiO$_2$ powders from 10 nm to 36 000 nm and measure their corresponding tan $\delta \sim f$ plots. Figure 3 shows some representative plots for different shear oscillation strain amplitudes. These curves clearly illustrate the evolution of the resonant system frequency with the increment of oscillation strain amplitude, from which we could obtain the dependence of elasticity on the oscillation strain amplitude as shown in Fig. 4. It is very interesting to note that the curve for the dependence of elasticity on the shear oscillation strain can be readily divided into four regimes according to their corresponding slopes, which we call elastic solid, plastic solid, viscoelastic solid, and viscous fluid, respectively.

As seen from Fig. 4, in the viscous fluid regime, where the amplitude of oscillation strain A_d is larger than a critical value A_d^c (~20 000 nm) but less than the average diameter of SiO$_2$ grains, the assembly of SiO$_2$ powders behaves as a viscous fluid displaying a viscous resistance instead of an elastic force, which lowers the system resonant frequency in
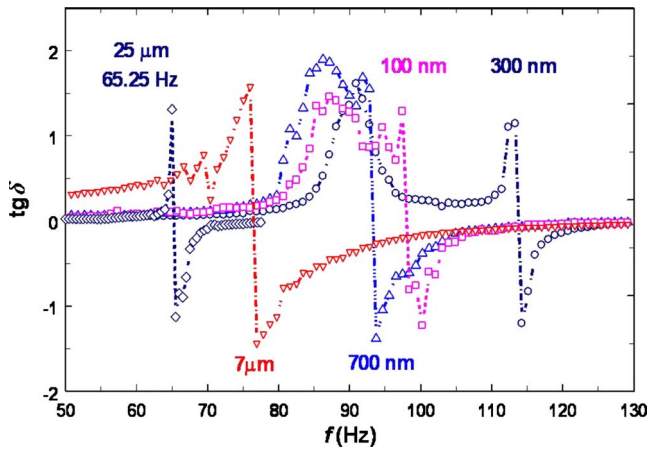
FIG. 3. (Color online) Frequency dependence of apparent internal frictions tan δ measured at different shear oscillation strain amplitudes. While the shear oscillation strain amplitude is 100, 300, 700 nm, 7, and 25 μm, the resonant frequencies of the system is 98.5, 113.7, 93.5, 76.5, and 65.25 Hz, respectively.

comparison to that of the unloaded system. This scenario is consistent with our familiar fluid state for strongly sheared granular material [1(a)]. However, while the oscillation strain amplitude is smaller than the critical value A_d^c, the assembly of SiO_2 powders displays an elastic force, making the system resonance frequency larger than that of the unloaded system. At the same time, the elastic coefficient shows strong dependence of oscillation shear strain amplitude.

How to understand above phenomena? As we know, the assembly of SiO_2 powders in the container of the Couette-like setup has a stress network inside due to its gravity and many stress chains are terminated on the side surfaces of the rotational cylinder. When the cylinder undergoes an oscillation rotation, the grains adhered on the cylinder surface impose certain shear oscillation strains onto their corresponding grain chains, which originally carry stress chains. For the simplicity of discussion, let us consider the effect of the shear strain applied onto a chain of SiO_2 grains, one stress chain inside the stress network, as shown in Fig. 5. While a shear strain is applied to the chain of SiO_2 grains, SiO_2
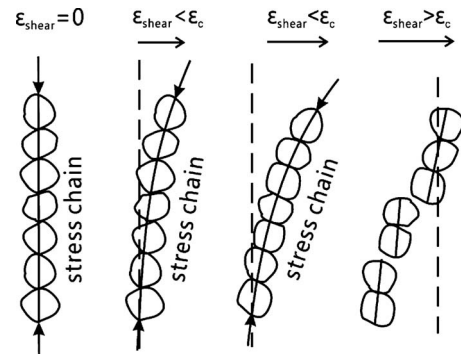

FIG. 4. (Color online) Dependence of elastic coefficient of the assembly of SiO_2 powders on the shear oscillation strain amplitude.

FIG. 5. Schematic diagram of the evolution of a stress chain of SiO_2 grains with the increase in imposed shear strain (ε_r represents the critical shear strain).

grains inside adjust their relative places to maintain their mechanical balances. So the SiO_2 grains will take some transversal motions to adjust their positions and to bear the shear strain. Because the SiO_2 grains are irregular, the small adjustments of the SiO_2 grains could be adopted in the SiO_2 grain chain without causing the collapse of the stress chain, which is termed self-lock [10]. However, the original configuration of the SiO_2 grain chain is favored by the free energy, so while the strain decreases, the original configuration will be recovered, i.e., the SiO_2 grain chain behaves like a spring displaying a restoring force, i.e., elastic force, while subject to a shear oscillation strain. This scenario could qualitatively explain the elastic force we observe in above experiments.

When the applied strain is increased, the adjustment (transversal motion) of the grains inside the chain is too large, resulting in the collapse of the stress chain, which implies that there is a critical value for the shear strain. Inside the assembly of SiO_2 powders, each stress chain has its own critical shear strain. So the stress distribution [11] inside the assembly of SiO_2 powders implies that the critical shear strain also has a distribution. In the regime of elastic solid of Fig. 4, the elastic force increases with the oscillation strain amplitude, which implies that all the stress chains inside could adopt the imposed oscillation strain and act like an elastic solid. However, one puzzle arises. Why does the elastic coefficient increase with oscillation strain amplitude rather than keep constant as like a normal solid? We have to resort to the fact that the restoring force originates from the interaction (e.g., static friction force) between SiO_2 grains in the stress chains, which depends on their relative configurations of SiO_2 grains. So the corresponding SiO_2 chains are not realistic normal spring with a constant elastic coefficient. And the increment of the elastic coefficient with the oscillation strain amplitude is one of the distinctive features, which is observed in our experiment.

When the shear oscillation strain is larger than 300 nm, the elastic coefficient begins to decrease, which means that some stress chains cannot stand the shear strain and break down. Thus the assembly of SiO_2 powders is in the state of plastic solid or viscoelastic solid, which has a different slope for the plot of elastic coefficient versus shear oscillation strain amplitude, as shown in Fig. 4. In plastic solid, the
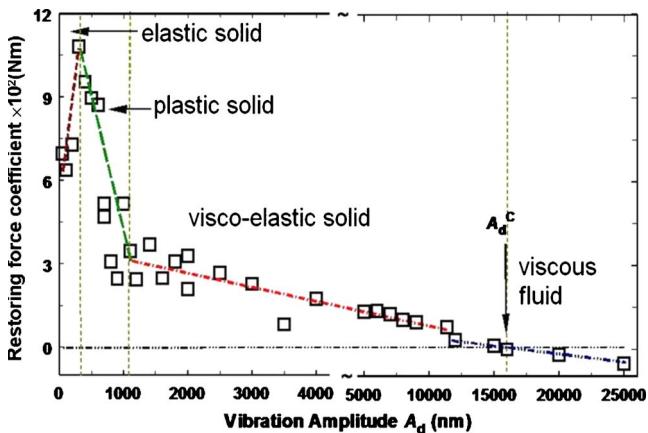
elastic coefficient decreases much faster than that in viscoelastic solid, from which we could infer that the distribution of critical shear strains is not uniform and most critical shear strains are less than 1200 nm, which is consistent with the fact that the distribution of stress inside granular material is not symmetric [11]. When the shear oscillation strain is increased up to 20 000 nm, almost all of the stress chains could not stand the shear oscillation strain and collapse. Then the assembly behaves like a fluid and is termed viscous fluid.

In conclusion we investigate the elasticity of granular material under shear oscillation strain by examining the variance of system resonant frequency of our developed viscoelastic spectroscope. In the presence of an assembly of SiO_2 powders, the system resonant frequency changes with the shear oscillation strain amplitude, from which we obtain the shear oscillation strain amplitude dependence of the elastic coefficient for the assembly of SiO_2 powders and we infer that under small shear oscillation strain the assembly of SiO_2 powders displays four different states: elastic solid, plastic solid, viscoelastic solid, and viscous fluid states respectively. The distribution of critical shear strains for the stress network is proposed to explain the dynamic behavior of the assembly of SiO_2 powders, which determines its state under shear oscillation strain.

[1] (a) H. M. Jaeger, S. R. Nagel, and R. P. Behringer, Rev. Mod. Phys. **68**, 1259 (1996); (b) J. R. Royer, D. J. Evans, L. Oyarte, Q. Guo, E. Kapit, M. E. Möbius, S. R. Waitukaitis, and H. M. Jaeger, Nature **459**, 1110 (2009); (c) M. G. Clerc, P. Cordero, J. Dunstan, K. Huff, N. Mujica, D. Risso, and G. Varas, Nat. Phys. **4**, 249 (2008).

[2] J. H. Snoeijer, M. van Hecke, E. Somfai, and W. van Saarloos, Phys. Rev. E **70**, 011301 (2004).

[3] C. S. O'Hern, S. A. Langer, A. J. Liu, and S. R. Nagel, Phys. Rev. Lett. **86**, 111 (2001).

[4] Y. Z. Wang, X. M. Xiong, and J. X. Zhang, J. Rheol. **52**, 999 (2008).

[5] J. X. Zhang, Y. Z. Wang, and X. M. Xiong, Chinese Patent No. 10122113A (7/16/2008).

[6] A. S. Nowick and B. S. Berry, *Anelastic Relaxation in Crystalline Solids: Appendix C* (Academic Press, New York, 1972).

[7] Y. Z. Wang, B. H. Li, X. M. Xiong, and J. X. Zhang, Rheol. Acta (to be published).

[8] K. To, P.-Y. Lai, and H. K. Pak, Phys. Rev. Lett. **86**, 71 (2001).

[9] E. R. Nowak, J. B. Knight, E. Ben-Naim, H. M. Jaeger, and S. R. Nagel, Phys. Rev. E **57**, 1971 (1998).

[10] J. Duran, E. Kolb, and L. Vanel, Phys. Rev. E **58**, 805 (1998).

[11] G. Løvoll, K. J. Måløy, and E. G. Flekkøy, Phys. Rev. E **60**, 5872 (1999).